Arabian Journal of Geosciences (2020) 13: 415
https://doi.org/10.1007/s12517-020-05420-9

ORIGINAL PAPER

Establishment of natural radioactivity baseline, mapping, and radiological hazard assessment in soils of Al-Qassim, Al-Ghat, Al-Zulfi, and Al-Majmaah

Thamer Alharbi [1]

Received: 29 August 2019 / Accepted: 1 May 2020 / Published online: 30 May 2020

Abstract
Radionuclide species comprising the primordial radioactive decay chains lead by ^{232}Th and ^{238}U, along with their associated daughter and granddaughter decay series, constitute a major fraction of the naturally occurring radioactive material (NORM). Gamma-ray radiation emitted by the decay of these NORMs, along with the ^{40}K in the soil, is mainly responsible for the human exposure to external gamma-rays. The radioactivity concentrations in soil samples collected from 138 sites have been determined as part of a survey to produce a radiological map of AL-Qassim, Al-Ghat, Al-Majmaah, and Al-Zulfi regions in the Kingdom of Saudi Arabia. The estimated mean values of ^{238}U, ^{232}Th, ^{40}K, ^{226}Ra, and gross α and β activities in the samples were 23.8 ± 11.61, 24.33 ± 17.63, 790 ± 398, 22.83 ± 11.70, 375 ± 205, and 734 ± 344 Bq kg^{-1}, respectively. The radiological risk indices related to the natural radioactivity in the soil samples, i.e., the absorbed dose rate in air, radium equivalent activity, and annual effective dose rate, were estimated to be 58.88 ± 29.21 nGy h^{-1}, 117.1 ± 59.65 Bq kg^{-1}, and 0.07 ± 0.04 mSv year^{-1}, respectively. The determined internal hazard index of the samples ranged from 0.07 to 1.45, with an estimated mean value of 0.4 ± 0.2. The radon concentration in the soil gas ranged from 39 to 508 Bq m^{-3}, with a mean value of 145.0 ± 52.9 Bq m^{-3}.

Keywords Soil · Natural radionuclides · ^{222}Rn soil gas · Gross α and β · Risk assessment

Introduction

The measurement of naturally occurring radioactive materials (NORMs) in environmental samples has received increasing attention recently. This is primarily because of the concern about human exposure resulting from the radioactive contamination of the environment. The environmental radiation background is a representation of the natural radioisotopes of ^{238}U, ^{232}Th, primordial ^{40}K, and other artificial radionuclides such as ^{137}Cs. Natural radiation accounts for approximately 85% of the human effective dose (UNSCEAR 2000; IAEA 1996). Its presence at certain levels can affect the human body, depending on location and geological characteristics. The activity levels of these radionuclides can be determined by a gamma radiation hazards assessment. The natural radiation to which the human body is exposed mainly originates from the decay of radium isotope (^{226}Ra), which produces radon gas (^{222}Rn) and its decay progeny (Yuvi 1988; Abdullahi et al. 2019). Radon is a noble gas that appears in different geological formations such as soil, rocks, the earth's crust, and building materials. The local environmental radon level is mainly determined by the radon exhalation rate from the soil, and the content of ^{226}Ra in soil plays an important role in the accumulation of ^{222}Rn gas in the outdoor and indoor environments. However, ^{226}Ra and ^{222}Rn are the decay products of ^{238}U with an estimated average of 2.7 mg kg^{-1} (Lide 1994). Therefore, environmental radiation background surveys are important for understanding radiological and geological characteristics, and also for identifying the biochemical and geochemical traces in the environment. Gross α and gross β activities in environmental samples (e.g., rocks, sand, soil, and water) have attracted considerable attention in recent years, because our living environment has been contaminated by natural radionuclides. Furthermore, elevated levels of β radiation may be a sign of the accidental atmospheric release of radioactivity from the Chernobyl nuclear reactor or nuclear

Responsible Editor: Amjad Kallel

✉ Thamer Alharbi
t.alharbi@mu.edu.sa

[1] Department of Physics, College of Science in Zulfi, Majmaah University, Majmaah 11952, Saudi Arabia

test explosions. The total radioactivity of α emitters in the soil of a particular area determines the area's gross α activity, which depends on geological formations, mineral distribution, and the type of activities in the selected area.

An artificial radioactive element such as cesium is produced in nuclear power plants and disposed in wastewater. The Fukushima Daiichi nuclear power plant accident in Japan increased the activity concentrations of ^{134}Cs and ^{137}Cs, with the respective half-lives of 2.06 and 30.4 years, in the soil, air, and water to dangerous levels (Shizuma et al. 2018). Several studies have described successful methods for removing radioactive elements such as cesium (^{134}Cs and ^{137}Cs) and cobalt (Co(II)) from nuclear wastewater. These studies involved the development of ligand-based nanomaterials such as mesoporous silica and conjugate adsorbent (Awual at al. 2014a), inorganic and conjugate adsorbent (Awual et al. 2014b), DSDH ligand (Shahat et al. 2015), nano-conjugate adsorbent (Awual et al. 2015), organic–inorganic mesoporous hybrid (Awual et al. 2016a), crown ether-based mesoporous adsorbent (Awual 2016), Schiff base ligand (Awual et al. 2017), and macrocyclic ligand (Awual et al. 2016b).

No study has yet reported the levels of natural radioactivity in the soils of the Al-Qassim, Al-Ghat, Al-Majmaah, and Al-Zulfi regions of Saudi Arabia. The present study aimed to estimate the natural radioactivity concentrations, radon concentrations, and gross α and β activities in these regions and to provide a radiation map as a reference for future radiological evaluations. The activity concentrations of ^{238}U, ^{226}Ra, ^{232}Th, and ^{40}K in 138 soil samples across the four regions were determined and then used to estimate the associated radiological hazards. The measurements were performed using a high-purity germanium (HPGe) gamma-ray detector. The gross α and β activities in the soil samples were estimated using low-background proportional detectors. The radiological hazards and risk assessment due to naturally occurring radionuclides (^{232}Th, ^{226}Ra, and ^{40}K) in the samples were estimated and compared with available results from other countries.

Materials and methods

Geology of the study area

This study was conducted in four different regions (Al-Qassim, Al-Ghat, Al-Majmaah, and Al-Zulfi) of Saudi Arabia. The study regions (latitude 24–27° N and longitude 41–44° E) are located in the center of the Arabian Peninsula, north-west of Riyadh, and have a population of 1.9 million (Fig. 1). The geology of the study area is not uniform; it consists of sand, clay, and limestone. The

Fig. 1 The map of Saudi Arabia showing the study area

Rummah Valley or Wadi Rummah, which has various dry riverbeds, crosses the entire Al-Qassim region and is one of the longest valleys in the Arabian Peninsula, covering a distance of over 600 km starting from the west near Medina to the border of Kuwait in the north-east of the Arabian Peninsula. In the Al-Qassim province, the soil consists of loose deposits in its natural state, but it can be compacted to attain relatively high, dry densities (Al-Refeai and Al-Ghamdy 1994).

Sample collection and preparation

There are several approaches for collection of soil samples include random, judgmental, stratified random, systematic random grid, systematic grid, search, and transect sampling (IAEA 2004). After field visit, the most suitable approach for the current study is systematic random grid due to some restrictions of sample collections in some grid points. The total area of the Al-Qassim province, Al-Ghat, Al-Majmaah, and Al-Zulfi was subdivided using square grids, and the soil samples were collected from within each cell using the random selection procedures. Soil samples were collected from 138 different sites at a depth of 0.2–0.3 m from ground level to obtain undistributed and pure soil samples from the four study regions, as shown in Fig. 2. Approximately 2–3 kg of soil from each location was collected in a polyethylene bag. The samples were sieved using a 2-mm mesh to remove unwanted materials. The samples were then dried in an oven at 90 °C for 24 h to remove any moisture. Additional sieving was performed using a 500-μm sieving machine (Octagon digital) to achieve homogeneity between samples. The dried, sieved samples were weighed and transferred into Marinelli beakers (500 mL) and sealed with adhesive tape. The beakers were then stored for 30 days to achieve secular equilibrium between radium (^{226}Ra) and radon (^{222}Rn) and radon's most abundant daughter products.

To measure the gross α and β activities, approximately 2 g of each dried sample was placed on a 5.08-cm-diameter stainless-steel planchet, and a small amount of UHU glue diluted with acetone was spread over the sample surface. The planchets were then kept under an infrared lamp for a few hours until the samples were fully glued.

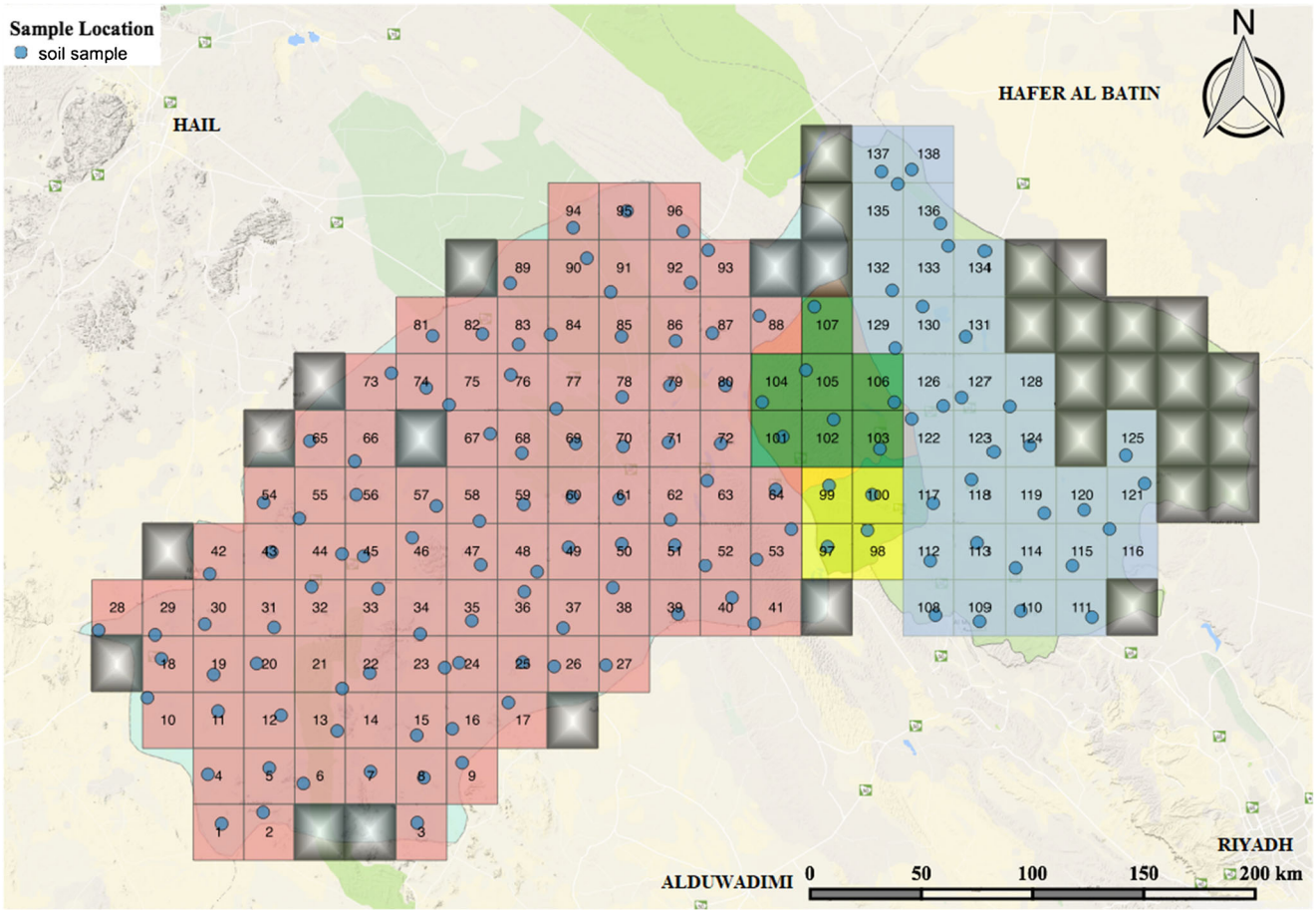

Fig. 2 Location of sampling points (blue circles) and study regions: Al-Qassim (red), Al-Zulfi (green), Al-Ghat (yellow), Al-Majmaah (blue), and unmeasured areas (gray).

Experimental technique

The activity concentration of radionuclides in the soil samples was determined by using a gamma-ray spectrometry technique. The gamma-ray spectrometry system comprised a high-resolution (n-type) HPGe coaxial detector (ORTEC) with a pre-amplifier, amplifier, high-voltage power supply, and multi-channel analyzer (MCA) coupled to a PC. To reduce the thermally induced leakage current, the HPGe detector was cooled using an X-COOLER system (ORTEC). The HPGe detector was placed in a 10-cm-thick cylindrical Pb shielding that was internally lined with a sheet of Cu (1.6 mm) and Sb (0.5 mm) to reduce the external gamma-ray radiation background in the measured spectrum. The HPGe detector efficiency curve based on the experimental data was calculated from the following equation:

$$\varepsilon_c = \frac{N_c}{t_c \times A_c \times P_\gamma},$$

where ε_c is the photopeak efficiency corresponding to a specific radionuclide, N_c is the net count in the photopeak, t_c is the measurement time (s) of the calibration source, A_c is the present activity of the source, and P_γ is the probability of γ-emission of the radionuclide. The energy resolution (FWHM) of the spectrometer was 0.8 keV and 2.2 keV for the 122-keV ^{57}Co and 1332-keV ^{60}Co gamma-ray lines, respectively. The energy and efficiency calibrations of the detector were performed using a mixed radionuclide source of ^{210}Pb, ^{88}Y, ^{241}Am, ^{137}Cs, ^{57}Co, ^{109}Cd, ^{139}Ce, ^{203}Hg, ^{113}Sn, ^{60}Co, and ^{85}Sr. The source was kept inside a 500-ml Marinelli beaker with the same geometry as that used for sample measurements. The efficiencies and activities were determined from the counts in the photopeak of the specific nuclides using the gamma vision software. Each soil sample was counted for 60,000 s. The background spectra, which were subtracted from the sample spectra, were collected for 48 h using deionized water in the Marinelli beaker.

Activity concentration determination by gamma-ray spectroscopy

The activity concentration of ^{226}Ra was calculated from the gamma-ray lines of energies 338.3, 911.1, and 969.11 keV (^{228}Ac); 609.3 keV (^{214}Bi); and 351.9 keV (^{214}Pb). The gamma-ray lines of 238.63 keV (^{212}Pb), 727.3 keV (^{212}Bi), and 583.19 keV (^{208}Tl) were used to determine the activity concentration of ^{232}Th. The gamma-ray photopeaks at 661.6 keV and 1460.8 keV were used to determine the activity concentrations of ^{137}Cs and ^{40}K, respectively. The minimum detectable activities (MDAs) for the soil samples were 0.40 ± 0.12 Bg kg^{-1} for ^{226}Ra, 0.32 ± 0.08 Bg kg^{-1} for ^{232}Th, 1.68 ± 0.52 Bg kg^{-1} for ^{40}K, and 0.03 ± 0.02 Bg kg^{-1} for ^{137}Cs. The activity concentrations of

Table 1 Range and average values of radionuclide (^{238}U, ^{226}Ra, ^{232}Th, and ^{40}K) concentrations, radon concentration, and gross α and gross β activities in the soil samples of the selected regions

Region	Sample No.		Activity concentration (Bq kg^{-1})				^{222}Rn (Bq m^{-3})	Gross α (Bq kg^{-1})	Gross β (Bq kg^{-1})
			^{238}U	^{226}Ra	^{232}Th	^{40}K			
Al-Qassim	1–96	Range	7.87–103.60	9.53–110.50	9.51–149.17	341.10–1550.91	79.2–508	96.70–1546.64	222.97–1651.32
		Average	26.66 ± 12.11	25.85 ± 11.97	28.98 ± 19.10	981.08 ± 320.72	154.6 ± 51.6	427.85 ± 219.63	877.91 ± 313.20
Al-Ghat	97–100	Range	8–14.50	7.77–11.23	8.30–10.66	341.01–455.4	69.0–102.7	119–246.18	320.11–375.3
		Average	12.24 ± 3	9.47 ± 1.44	9.32 ± 1.07	375.98 ± 53.33	86.0 ± 16.0	185.97 ± 61.80	346.60 ± 24.65
Al-Zulfi	101–107	Range	8.67–30.02	8.57–25.70	8.56–25.87	284.40–485.78	75.3–160.3	67–349.64	273.75–475.21
		Average	16.96 ± 7.06	14.08 ± 6.07	13.84 ± 6.08	371.27 ± 70.91	106.3 ± 29.7	259.27 ± 106.08	374.72 ± 76.96
Al-Majmaah	108–138	Range	6.24–29.97	6.01–33.77	6.28–22.64	11.64–534.26	39.0–256.6	29.72–390.23	146.37–558.53
		Average	17.97 ± 7.10	17.19 ± 7.68	14.25 ± 5.33	347.18 ± 124.32	116.4 ± 47.6	264.44 ± 89.30	422.45 ± 110.57
All regions	1–138	Average	23.80 ± 11.61	23.83 ± 11.70	24.33 ± 17.63	790.21 ± 398.64	145.0 ± 52.9	375 ± 205	734 ± 344

Table 2 Comparison between the levels of ^{238}U, ^{232}Th, and ^{40}K in the soil samples and available data for other countries

Country	^{238}U (Bg kg^{-1})	^{232}Th (Bg kg^{-1})	^{40}K (Bg kg^{-1})	References
Algeria	30 (2–110)	25 (2–140)	370 (66–1150)	UNSCEAR (2000)
Egypt	37 (6–120)	18 (2–96)	320 (29–650)	UNSCEAR (2000)
India	29 (7–81)	64 (14–160)	400 (38–760)	UNSCEAR (2000)
Malaysia	66 (49–86)	82 (63–110)	310 (170–430)	UNSCEAR (2000)
Syria	23 (10–64)	20 (10–32)	270 (87–780)	UNSCEAR (2000)
Iraq	39.54 (26.5–69)	19.85 (14.7–32.2)	329.38 (25.8–528.2)	NEA-OECD (1979)
Turkey	28 (6–73)	40 (7–151)	667 (87–2084)	Nordic (2000)
Iran	41 (21–65)	26 (15–45)	395 (146–500)	Fujiyoshi and Sawamura (2004)
Jordan	44.9 (30.3–59.9)	18.1 (14–20.8)	138.1 (31.3–251.5)	UNSCEAR (1988)
Kuwait	17.3 (5.9–32.3)	15.1 (3.5–27.3)	385 (74–698)	ICRP (1990)
Pakistan	49 (36.6–56.9)	62.4 (45.8–69.9)	670.6 (552.1–868.4)	Abdi et al. (2008)
Qatar	51.52 (14.97–213.9)	9.48 (4.55–13.17)	204 (111.4–249)	Saleh and Abu Shayeb (2014)
Saudi Arabia	23.80 (6.24–103.66)	24.33 (5.78–149.17)	790 (111–1550)	Present
Worldwide average	35 (16–110)	30 (11–64)	400 (140–850)	UNSCEAR (2000)

specific radioisotopes were determined using the following expression (Dovlete and Povinec 2004):

$$A = \frac{C_n}{\varepsilon_f P_\gamma t_s m},$$

where A is the activity concentration of a specific radionuclide in Bq kg^{-1}, C_n is the net count of the corresponding peak, P_γ is the absolute emission probability for a specific gamma-ray energy, ε_n is the absolute energy efficiency, m is the mass of the sample in kg, and t_s is the counting time in s.

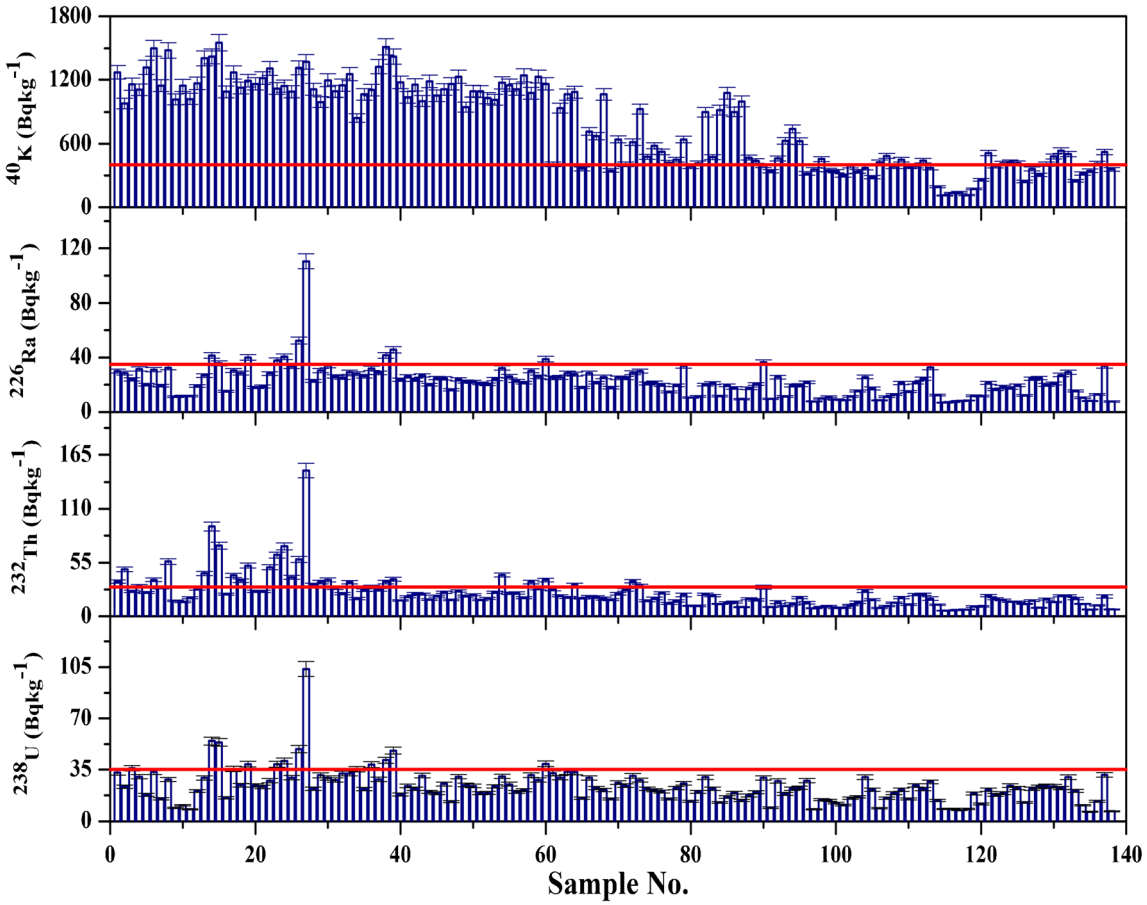

Fig. 3 Activity concentration distributions of ^{238}U, ^{232}Th, ^{226}Ra, and ^{40}K in the soil samples; red lines represent worldwide average values

Determination of radon concentration

The radon (^{222}Rn) concentration of the sampling locations was measured using a RAD7 semiconductor-based detector connected to a soil gas probe. At each sampling location, the stainless-steel probe, with holes near the tip, was immersed in the soil to a depth of 1 m. The probe was connected to the RAD7 detector with a desiccant tube, followed by inert filters for absorbing the soil gas. The counting time was 30 min for each location (Durridge Co 2017; Thu et al. 2019).

Gross α and β activity measurements by proportional counting system

An advanced low-background α/β proportional system (LB4200, CANBERRA) was used to determine the gross α and β activities. The multi-detector counting system was equipped with 16 gas flow proportional detectors using a mixed P10 gas (90% Ar and 10% CH_4). The system was calibrated simultaneously using disk-shaped standard sources (^{90}Sr for β and ^{241}Am for α particles). The counting efficiency of the low-background proportional counting system was found to be 2.94% for α particles (based on the guaranteed reagent U_3O_8 standard) and 28.92% for β particles (based on the high-purity reagent KCl standard) using 2 g of the standard reference sample. The background and samples were counted for 24 h. For the soil samples, the MDAs were 0.11 Bg kg^{-1} for gross α and 0.16 Bg kg^{-1} for gross β.

Radiological risk assessment

The specific activity concentrations of the ^{226}Ra, ^{232}Th, and ^{40}K nuclides were used to estimate the outdoor external dose rates for the measured samples. The internal hazard index (H_{int}), external hazard index (H_{ext}), radium equivalent activity (Ra_{eq}), and annual effective dose rate equivalent (AEDE) were calculated using the following equations (Berekta and Mathew 1985; UNSCEAR 2008):

$$Ra_{eq} = A_U + (A_{Th} \times 1.43) + (A_K \times 0.077)$$

$$DR = (0.462 \times A_U) + (0.604 \times A_{Th}) + (0.0417 \times A_K)$$

$$\mathrm{AEDE} = \mathrm{D} \times 1.23 \times \frac{10^{-3} mSv}{y}$$

$$\mathrm{H_{int}} = \left(\frac{A_U}{185} + \frac{A_{Th}}{259} + \frac{A_K}{4810}\right),$$

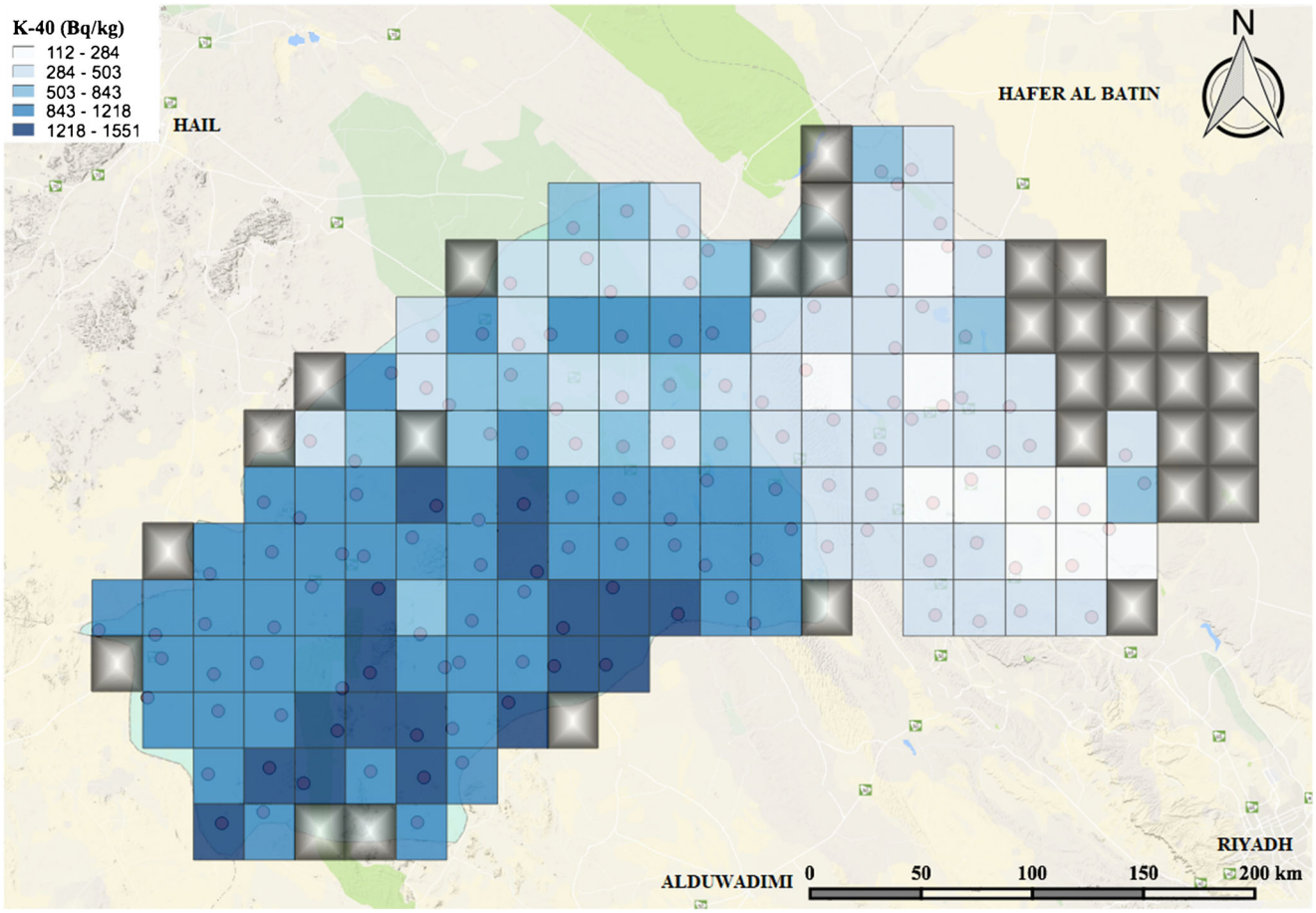

Fig. 4 Radiation map of activity concentration distributions of ^{40}K for selected regions (Al-Qassim province, Al-Ghat, Al-Zulfi, and Al-Majmaah)

where DR is the absorbed dose rate in nGy h^{-1} in the air 1 m above the ground surface; Ra_{eq} is in Bq kg^{-1}; AEDE is in mSv $year^{-1}$; and A_U, A_{Th}, and A_K are the activity concentrations of ^{238}U, ^{232}Th, and ^{40}K in Bq kg^{-1} in the soil samples, respectively.

Results and discussion

Radionuclides concentration

Table 1 lists the range of activity concentrations and average activity concentrations of the ^{238}U, ^{232}Th, ^{226}Ra, and ^{40}K nuclides for all soil samples. The overall average activity concentrations of ^{238}U, ^{232}Th, and ^{226}Ra in the soil samples were 23.80 ± 11.61, 24.33 ± 17.63, and 23.83 ± 11.70 Bq kg^{-1}, respectively. These average activity concentrations are lower than the worldwide average values of 35, 30, and 35 Bq kg^{-1}, respectively, whereas for ^{40}K, the mean activity concentration was found to be 790 ± 398 Bq kg^{-1}, which exceeds the worldwide average of 400 Bq kg^{-1} (UNSCEAR 2000). The activity concentrations of ^{238}U, ^{232}Th, ^{226}Ra, and ^{40}K at the sampling points in the Al-Qassim region were higher compared with those in the other three regions (Al-Ghat, Al-Zulfi, and Al-Majmaah). This may be caused by the heavy mineral groups from the Paleozoic Era that are dominated by the ultra-stable minerals zircon, tourmaline, and rutile in the Al-Qassim region. Other heavy minerals, including garnet, monazite, staurolite, and kyanite, were also found in small quantities. Among light minerals, alkali feldspars were more abundant than plagioclase, owing to the significantly higher K_2O concentrations, controlled by the presence of K-feldspar, K-mica, and glauconite (Bassis et al. 2016). The activity levels of ^{238}U, ^{232}Th, and ^{40}K in the soil samples are compared with those from other countries in Table 2. The variations in the activity levels can be explained by the differences in geological and geographical conditions, as well as by the geochemical characteristics. Figure 3 shows the activity concentration distributions of ^{238}U, ^{232}Th, ^{226}Ra, and ^{40}K in each soil sample compared with their worldwide average values, indicated by red lines.

Figure 4 shows the distribution of the measured activity levels of ^{40}K from the present work. The highest activities were found in the southwestern Al-Qassim region, and it is clear that its activity decreases from west to east. The maximum concentration of ^{40}K found in this work was below the highest worldwide concentration. The high levels of ^{40}K concentrations in the south-west region may be attributable to the

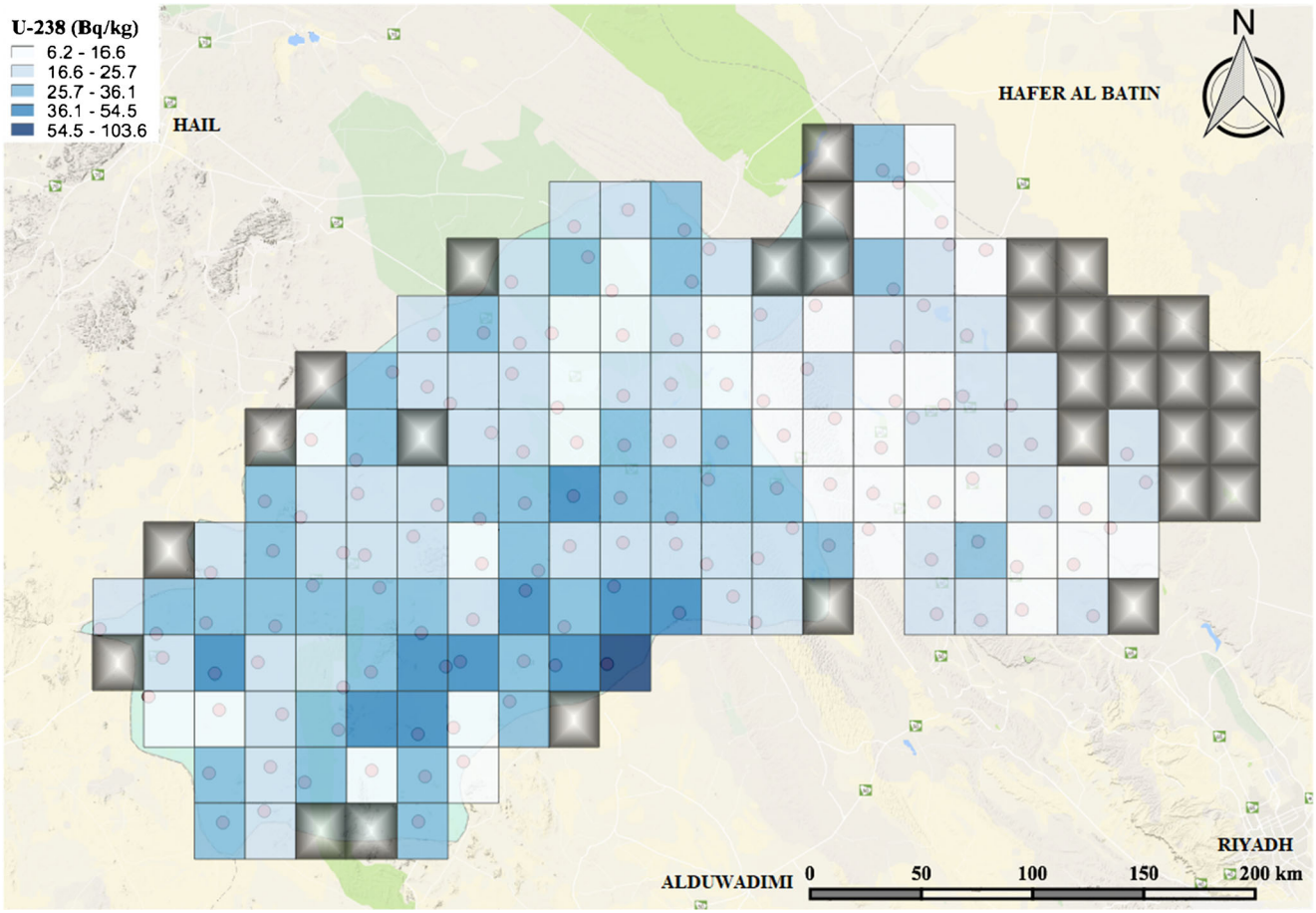

Fig. 5 Radiation map of activity concentration distributions of ^{238}U for selected regions (Al-Qassim province, Al-Ghat, Al-Zulfi, and Al-Majmaah)

high content of heavy and lighter minerals in red to pink sedimentary rocks and partially micaceous silty sandstones. Moreover, there are various dry riverbeds, many crossing the entire region from the west to the north-east (Al-Refeai and Al-Ghamdy 1994; Abu Shayeb et al. 2017).

The results from the activity concentration measurements were used to generate a radiological map of the selected regions (138 sampling points), as depicted in Figs. 4, 5, 6, 7 for ^{40}K, ^{238}U, ^{226}Ra, and ^{232}Th, respectively. The activity distribution of ^{40}K, ^{238}U, ^{226}Ra, and ^{232}Th of the selected regions was decreased in a way west-south > north-west > north-east > east-south. However, radionuclide concentrations in the south-west region of Al-Qassim were higher than those in the other regions due to being highly enriched in zircon (Bassis et al. 2016). Benaafi and Abdullatif (2015) reported that the mineralogical composition of the sand dunes in the Al-Qassim region has a high percentage of SiO_2 (quartz) and a very low percentage of feldspars. However, in some areas, feldspars and calcite were found significant minerals. A reasonable hypothesis would be that uranium, thorium, and potassium-enriched crystallinity is the main source of heavy and lighter minerals in the sandstones or sedimentary rocks of the Al-Qassim region during the Ordovician age (Pitkin and Huffman 1986).

The measured activity concentrations were correlated for all samples for ^{238}U/^{226}Ra and ^{232}Th/^{226}Ra. The ratio of ^{238}U/^{226}Ra and ^{232}Th/^{226}Ra varied from 0.6 to 1.5 and 0.4 to 2.2, respectively. The average values of ^{238}U/^{226}Ra and ^{232}Th/^{226}Ra were 1.0 ± 0.2 and 1.1 ± 0.3 respectively. There is a slight variation in ^{232}Th/^{226}Ra activity ratios across the soil samples, which may be due to the fact that uranium or thorium has been absorbed by clay minerals or organic matters in soil.

Radon concentration

The range and average value of the radon (^{222}Rn) concentration in all soil sample locations from the present work are listed in Table 1. The measured ^{222}Rn concentration varied from 39 to 508 Bq m^{-3} with an average of 145.0 ± 52.9 Bq m^{-3}. The measured values are in agreement with the typical values (UNSCEAR 2000; Eisenbud and Gesell 1997). The levels of ^{222}Rn in the samples from the Al-Qassim region were higher than those from the other regions, which can be attributed to the different soil types and compact packing of the sandstones/bedrocks. Based on the Sweden Criteria radon hazard assessment (Lara et al. 2015), a radon activity concentration below 10 kBq m^{-3} is classified as "low risk," a

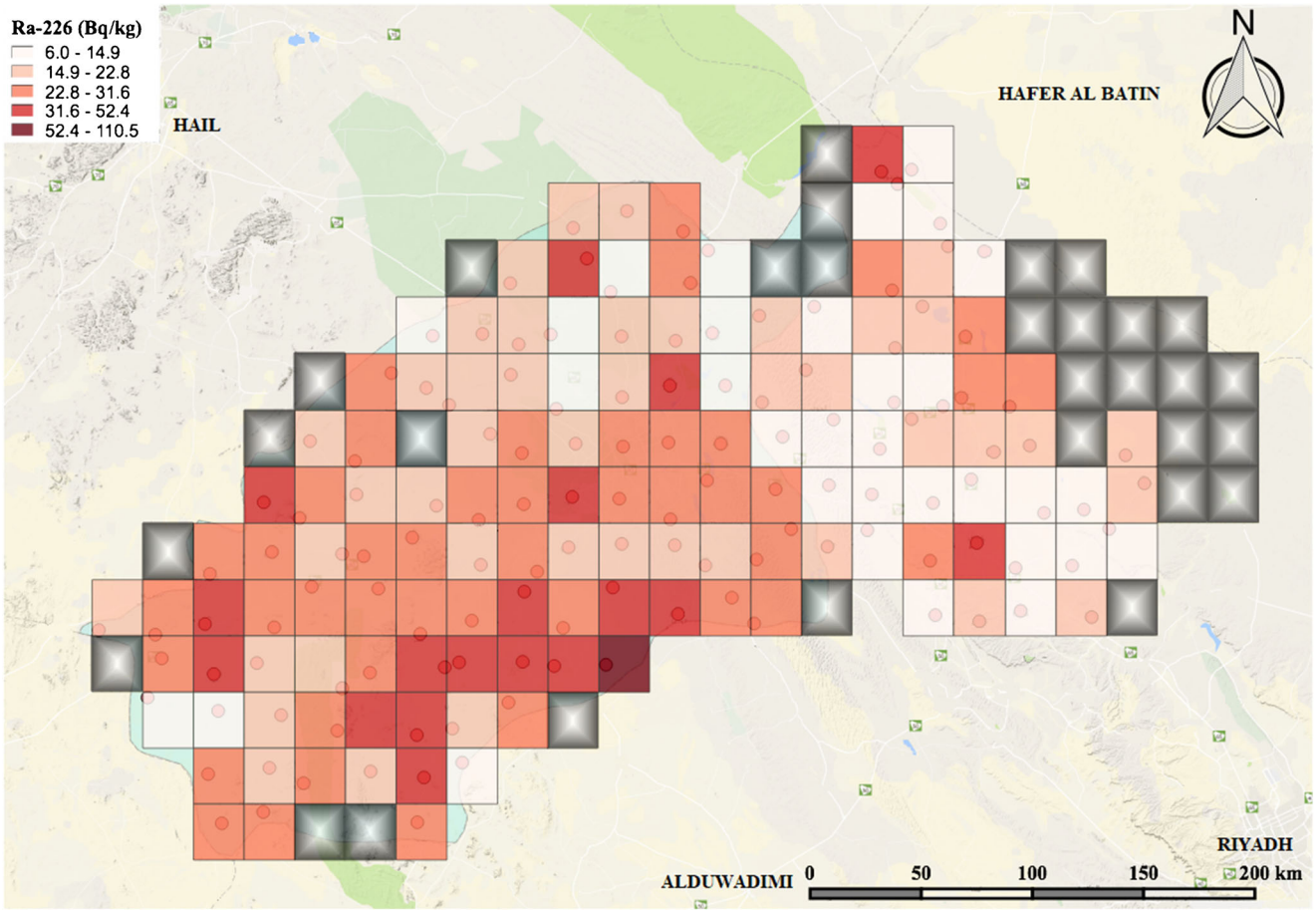

Fig. 6 Radiation map of activity concentration distributions of ^{226}Ra for selected regions (Al-Qassim province, Al-Ghat, Al-Zulfi, and Al-Majmaah)

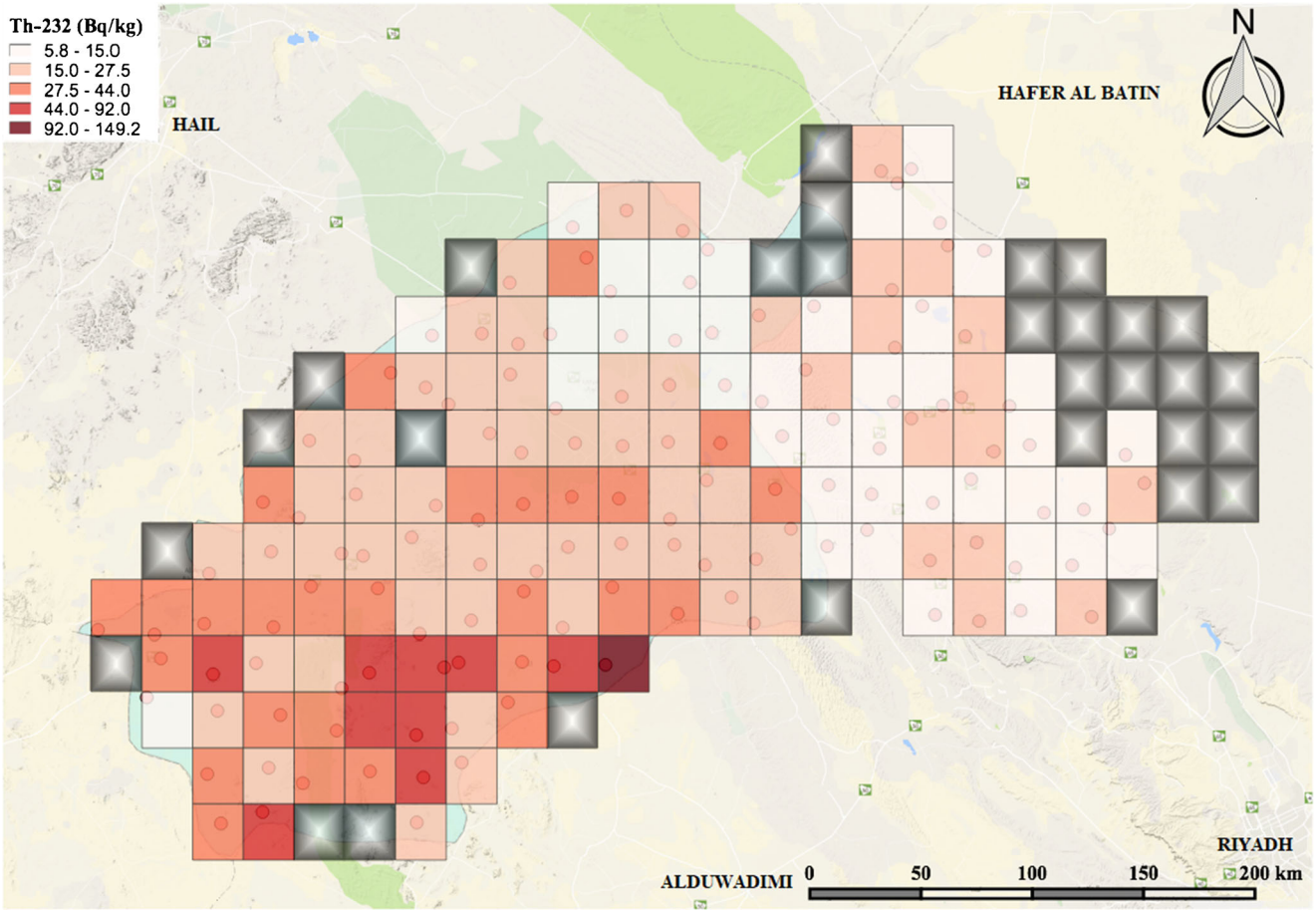

Fig. 7 Radiation map of activity concentration distributions of ^{232}Th for selected regions (Al-Qassim province, Al-Ghat, Al-Zulfi, and Al-Majmaah)

concentration between 10 and 50 kBq m^{-3} is classified as "normal risk," and a concentration greater than 50 kBq m^{-3} is classified as "high risk." Results from the current work show that all values classified as "low risk."

Gross α and gross β activities

The gross α and β activities of the samples from the selected regions are summarized in Table 1. The gross β activity in groundwater samples from the same regions (Al-Qassim, Al-Zulfi, and Al-Majmaah) was found to be approximately 5–100 times higher than the gross α activity, owing to the high concentrations of ^{228}Ra and ^{40}K, compared with the ^{226}Ra concentration (Alharbi et al. 2018). The gross α activity depends only on the levels of natural α-emitters (^{238}U, ^{234}U, ^{232}Th, ^{230}Th, ^{228}Th, ^{226}Ra, and ^{210}Po), while the gross β activity depends on the levels of natural β-emitters (^{228}Ra, ^{210}Pb, and ^{40}K). It was found that the levels of gross α and gross β activities at the sampling points of the Al-Qassim region were higher than those of the other three regions (Al-Ghat, Al-Zulfi,

Table 3 Comparison of the range of gross α and gross β activities in the soil samples with data from other countries

Country	Gross α (Bg kg^{-1})	Gross β (Bg kg^{-1})	References
Jordan (Ma'al)	3.17–29.25	634.01–1084	UNSCEAR (1988)
China (northeastern south sea)	119–212	884–1064	Alazemi et al. (2016)
Malaysia	15–9634	142–6173	Jabbar et al. (2010)
Macedonia	221–1360	438–1052	Al-Sulaiti et al. (2010)
Nigeria	48.5–64.0	411.5–2710.0	Zhou et al. (2015)
Vietnam	207–509	275–529	Lee et al. (2014)
Turkey	800–4713	73–11773	Lee et al. (2014)
Saudi Arabia	29.72–1546.64	146.37–1651.32	Present

Table 4 Radiological risk factors measured for all samples from the current work

	Ra_{eq} (Bg kg^{-1})	DR (nGy h^{-1})	AEDE (mSv $year^{-1}$)	H_{ext}	H_{int}
Worldwide					
Average value[a]	370	57	0.07	NA	NA
Range[a]	NA	18-93	NA	NA	NA
Present work					
Average value	117.1 ± 59.65	58.88 ± 29.21	0.07 ± 0.04	0.3 ± 0.2	0.4 ± 0.2
Minimum	23.6	11.05	0.01	0.1	0.1
Maximum	147.8	202.04	0.25	1.2	1.5

[a] UNSCEAR (2000)

and Al-Majmaah), which may be due to the high concentrations of ^{238}U, ^{235}U, ^{232}Th, ^{226}Ra, and ^{40}K found in this study. Table 3 compares the levels of gross α and gross β activities in the soil samples with those from other countries. The different ranges of gross α and gross β activities are due to the activity concentrations of uranium (^{234}U and ^{238}U), radium (^{226}Ra and ^{224}Ra), polonium (^{210}Po), lead (^{210}Pb), and potassium (^{40}K), which normally depend on the geological and geochemical characteristics of the soil.

Radiological hazards and risk assessment

The evaluated radiological risk indices for the soil samples from the present work are summarized in Table 4. The gamma-absorbed dose rate (DR) in the air 1 m above ground level is defined as the radiation dose received by a person from gamma-rays emitted by the radionuclides (^{232}Th, ^{226}Ra, ^{40}K, and ^{137}Cs) present in the soil. The DR values of the samples varied from 11.05 to 202.04 nGy h^{-1}, with an average value of 58.88 ± 29.21 nGy h^{-1}. Radium equivalent activity (Ra_{eq}) was used to assess the hazards associated with soil that contains ^{232}Th, ^{226}Ra, and ^{40}K; it is determined by assuming that 370 Bq kg^{-1} of ^{226}Ra, 260 Bq kg^{-1} of ^{232}Th, and 4810 Bq kg^{-1} of ^{40}K produce the same gamma dose rate (UNSCEAR 2000). The range of Ra_{eq} for the samples was 23.6–147.8 Bq kg^{-1}, with an average value of 118.48 ± 59.65 Bq kg^{-1}. H_{int} was used to evaluate the internal radiation exposure to the respiratory system through the inhalation of radioactive gasses (radon and thoron) and their short-lived daughter products, which emit α particles. The H_{int} values of the samples varied from 0.07 to 1.45 with an estimated mean value of 0.4 ± 0.2. H_{ext} was used to estimate the hazards due to exposure to gamma-ray radiation associated with the ^{232}Th, ^{226}Ra, and ^{40}K in soil. The H_{ext} values of the samples varied from 0.1 to 1.2, with an estimated mean value of 0.3 ± 0.2. The AEDE values of the samples ranged from 0.01 to 0.25 mSv $year^{-1}$, with an estimated average of 0.07 ± 0.04 mSv $year^{-1}$, which is below the maximum recommended worldwide level of 1 mSv $year^{-1}$ (UNSCEAR 2000).

Conclusion

The activity concentrations of radionuclides (^{238}U, ^{232}Th, ^{226}Ra, and ^{40}K) and a gamma radiation hazard assessment were obtained for 138 soil samples using an HPGe gamma-ray spectrometer. The average activity concentrations of ^{238}U, ^{232}Th, and ^{226}Ra in the samples were found to be lower than the worldwide average values, whereas the average activity of ^{40}K was much higher than the worldwide average value. The radon concentration from the sample locations was within the typical range and can be considered "low risk." A multi-detector low-background α/β counting system was used to determine the gross α and β activities in the samples, and the values obtained ranged from 29.72 ± 1.43 to 1546.64 ± 115.06 Bq kg^{-1} and 146.37 ± 24.95 to 1651.32 ± 44.15 Bq kg^{-1}, respectively. Finally, the radiological hazards associated with the natural radioactivity in the soil samples were estimated.

Acknowledgment The author gratefully acknowledges Dr. Naser Alazmi for making the radiological maps (Environmental Radiation Protection Laboratory, Kuwait) and Mr. Muzahir Ali Baloch (Physics Lecturer in the Majmaah University, Saudi Arabia) for sample preparation and data collection.

Funding information The author acknowledges the financial support provided by King Abdulaziz City for Science and Technology under project No. 35-37.

Compliance with ethical standards

Conflict of interest The author declares no conflict of interest.

References

Abdi MR, Kamali M, Vaezifar S (2008) Distribution of radioactive pollution of ^{238}U, ^{232}Th, ^{40}K and ^{137}Cs in northwestern coasts of Persian Gulf. Iran Mar Pollut Bull 56:751–757

Abdullahi S, Ismail AF, Samat S (2019) Radiological characterization of building materials used in Malaysia and assessment of external and internal doses. Nucl Sci Tech 30:46

Abu Shayeb M, Alharbi T, Baloch MA, Alsamhan RAO (2017) Transfer factors for natural radioactivity into date palm pits. J Environ Radioact 167:75–79

Alazemi N, Bajoga DA, Bradley DA, Regan PH, Shams H (2016) Soil radioactivity levels, radiological maps and risk assessment for the state of Kuwait. Chemosphere 154:55–62

Alharbi T, Adel A, Baloch MA, Alsagabi FS, Alssalim AY, Alslamah SA, Alkhomashi N (2018) Natural radioactivity measurements and age-dependent dose assessment in groundwater from Al-Zulfi, Al-Qassim and Al-Majmaah regions. Saudi Arabia J Radioanal Nucl Chem 318:935–945

Al-Refeai T, Al-Ghamdy D (1994) Geological and geotechnical aspects of Saudi Arabia. Geotech Geo Eng 12:253–276

Al-Sulaiti H, Regan PH, Bradley DA, Malain D, Santawamaitre T, Habib A, Matthews M, Bukhari S, Al-Dosari M (2010) A preliminary report on the determination of natural radioactivity levels of the State of Qatar using high-resolution gamma-ray spectrometry. Nucl Instr Meth Phys Res A 619:427–431

Awual MR (2016) Ring size dependent crown ether based mesoporous adsorbent for high cesium adsorption from wastewater. Chem Eng J 303:539–546

Awual MR, Yaita T, Taguchi T, Shiwaku H, Suzuki S, Okamoto Y (2014a) Selective cesium removal from radioactive liquid waste by crown ether immobilized new class conjugate adsorbent. J Hazard Mater 278:227–235

Awual MR, Miyazaki Y, Taguchi T, Shiwaku H, Yaita T (2014b) Radioactive cesium removal from nuclear wastewater by novel inorganic and conjugate adsorbents. Chem Eng J 242:127–135

Awual MR, Yaita T, Shiwaku H, Suzuki S (2015) A sensitive ligand embedded nano-conjugate adsorbent for effective cobalt(II) ions capturing from contaminated water. Chem Eng J 276:1–10

Awual MR, Miyazaki Y, Taguchi T, Shiwaku H, Yaita T (2016a) Encapsulation of cesium from contaminated water with highly selective facial organic–inorganic mesoporous hybrid adsorbent. Chem Eng J 291:128–137

Awual MR, Yaita T, Miyazaki Y, Matsumura D, Shiwaku H, Taguchi T (2016b) A reliable hybrid adsorbent for efficient radioactive cesium accumulation from contaminated wastewater. Sci Rep 6:19937

Awual MR, Alharthi NH, Hasan MM, Karim MR, Islam A, Znad H, Hossain MA, Halim ME, Rahman MM, Khaleque MA (2017) Inorganic-organic based novel nano-conjugate material for effective cobalt(II) ions capturing from wastewater. Chem Eng J 324:130–139

Bassis A, Hinderer M, Meinhold G (2016) New insights into the provenance of Saudi Arabian Palaeozoic sandstones from heavy mineral analysis and single-grain geochemistry. Sediment Geol 333:100–114

Benaafi M, Abdullatif O (2015) Sedimentological, mineralogical, and geochemical characterization of sand dunes in Saudi Arabia. Arab J Geosci 8:11073–11092

Berekta J, Mathew PJ (1985) Natural radioactivity of Australian building materials, industrial wastes and by-products. Health Phys 48:87–95

Dovlete C, Povinec PP (2004) Quantification of uncertainty in gamma-spectrometric analysis of environmental samples, IAEA-TECDOC-1401. Int At Energy Agency, Austria:103–126

Durridge Co (2017) User manual, RAD7 Radon Detector. https://durridge.com/.

Eisenbud M, Gesell T (1997) Environmental radioactivity: from natural, industrial and military sources, fourth edn. Academic Press, San Diego

Fujiyoshi R, Sawamura S (2004) Mesoscale variability of vertical profiles of environmental radionuclides (^{40}K, ^{226}Ra, ^{210}Pb and ^{137}Cs) in temperate forest soils in Germany. Sci Total Environ 320:177–188

IAEA (1996) Radiation safety. IAEA Division of Public Information, 00725 IAEA/PI/A47E. IAEA, Austria.

International Atomic Energy Agency (IAEA), Soil sampling for environmental contaminants. IAEA-TECDOC-1415. 2004, Vinna: IAEA.

ICRP (1990) International Commission on Radiological Protection; Recommendations of the International Commission on Radiological Protection, Publication 60 Ann. Pergamon Press, Oxford

Jabbar A, Arshed W, Bhatti SA, Ahmad SS, Rehman US, Dilband M (2010) Measurement of soil radioactivity levels and radiation hazard assessment in mid Rechna interfluvial region, Pakistan. J Radioanal Nucl Chem 283:371–378

Lara E, Rocha Z, Palmieri HEL, Santos TO, Rios FJ, Oliveira AH (2015) Radon concentration in soil gas and its correlations with pedologies, permeabilities and 226Ra content in the soil of the Metropolitan Region of Belo Horizonte-RMBH, Brazil. Radiat Phys Chem 116:317–320

Lee SK, Wagiran H, Ramli AT (2014) A survey of gross alpha and gross beta activity in soil samples in Kinta district, Perak, Malaysia. Radiat Prot Dosimetry 162:345–350

Lide DR (ed) (1994) Handbook of chemistry and physics, 74th edn. CRC, Boca Raton

Nordic (2000) Naturally occurring radiation in the Nordic countries recommendations. The Flag Book Series, ISBN:91-89230-00-0.

Pitkin AJ, Huffman CA (1986) Geophysical and geological investigations of aerial radiometric anomalies in the Paleozoic Tabuk Formation, in northwestern Saudi Arabia: a preliminary report. Report: 86−259, U.S. Geological Survey.

Saleh H, Abu Shayeb M (2014) Natural radioactivity distribution of southern part of Jordan (Ma'an) Soil. Ann Nucl Energy 65:184–189

Shahat A, Awual MR, Naushad M (2015) Functional ligand anchored nanomaterial based facial adsorbent for cobalt(II) detection and removal from water samples. Chem Eng J 271:155–163

Shizuma K, Fujikawa Y, Kurihara M, Sakurai Y (2018) Identification and temporal decrease of ^{137}Cs and ^{134}Cs in groundwater in Minami-Soma City following the accident at the Fukushima Dai-ichi nuclear power plant. J Environ Pollut 234:1–8

Thu HNP, Van Thang N, Loan TTH, Van Dong N, Hao LC (2019) Natural radioactivity and radon emanation coefficient in the soil of Nonh Son region, Vietnam. Applied Geochemistry 104:176–183

UNSCEAR (1988) Sources, effects and risks of ionizing radiation. United Nations Scientific Committee on the Effects of Atomic Radiation. United Nations Publication, New York, USA

UNSCEAR (2000) Sources and effects of ionizing radiation. United Nations Scientific Committee on the Effects of Atomic Radiation Report Vol. 1 to the general assembly with annexes, United Nations New York

UNSCEAR (2008) Sources and effects of ionizing radiation. United Nations Scientific Committee on the Effects of Atomic Radiation Report Vol. 1 to the general assembly with annexes, United Nations New York

Yuvi K (1988) Indoor air quality: radon report on a WHO working group. J Environ Radioact 8:73–91

Zhou P, Li D, Li H, Fang H, Huang C, Zhang Y, Zhang H, Zhao L, Zhou J, Wang H, Yang J (2015) Distribution of radionuclides in a marine sediment core off the waterspout of the nuclear power plants in Daya Bay, northeastern South China Sea. J Environ Radioact 145:102–112